

# Asphaltenes and Waxes Do Not Interact Synergistically and Coprecipitate in Solid Organic Deposits<sup>†</sup>

Xiaoli Yang<sup>‡</sup> and Peter Kilpatrick\*

Department of Chemical Engineering, North Carolina State University,  
Raleigh, North Carolina 27695-7905

Received January 20, 2005. Revised Manuscript Received May 12, 2005

Waxes and asphaltenes are the major components in organic deposits from petroleum fluids. A key unresolved issue is whether there are significant intermolecular interactions between wax and asphaltene molecules during precipitation that would lead to synergy and coprecipitation, i.e., the phase change of one class inducing the precipitation of the other class. To address this, we studied six organic deposits in great chemical and physical detail: three that we categorized as predominantly wax deposits, two that were asphaltenic deposits, and one that seemed to be an organic acid deposit. Chemical analyses included elemental analysis, Fourier transform infrared (FTIR) spectroscopy, high-temperature simulated distillation, melting range measurement, and solubility experiments, performed on both parent crude oils and their corresponding deposits. The wax deposits contain in excess of 44 wt % waxes, and the complement of the deposits was occluded oil, water, and inorganic solids. Less than 6.2% (w/w) of these deposits were asphaltenes. Waxy-deposit waxes have higher melting points, longer straight-chain methylene, higher carbon number distributions, and higher molecular weights than their parent crude waxes. Asphaltenic-deposit waxes have properties that are almost identical to their parent crude oil waxes. Asphaltenic deposits contained >27 wt % asphaltenes. The properties of asphaltenes isolated from asphaltenic deposits were compared with the properties of asphaltenes isolated from their parent crude oils. The metal content and apparent VPO molecular weight of asphaltenic-deposit asphaltenes are significantly higher than those of corresponding crude-oil asphaltenes. The solubility of asphaltenic-deposit asphaltenes is much lower than the solubility of asphaltenes from their parent crude oils. The results indicate that the asphaltenes in the wax deposits are likely a component of the occluded oil in the deposit. A key conclusion of our work is that there is no evidence for any intermolecular interaction between waxes and asphaltenes to suggest synergy in precipitation. In fact, the evidence very much points to only one of these components undergoing a phase change and precipitating in an organic deposit and the other component simply being a portion of the crude oil occluded in the deposit.

## 1. Introduction

Precipitation and deposition of organic solids—primarily asphaltenes and waxes—during the production, transportation, and processing of petroleum is common and poses a serious challenge to efficient operation.<sup>1–5</sup>

Waxes are a mixture of linear, branched, and cyclic aliphatic hydrocarbons isolated from petroleum. Most crude oils contain 1–30 wt % high-molecular-weight paraffin and microcrystalline waxes, which, at low temperatures, precipitate as a component in organic deposits.<sup>6,7</sup> Asphaltenes are a solubility class typically defined as the heptane-insoluble, toluene-soluble fraction of petroleum.<sup>8</sup> Asphaltenes possess a high degree of polynuclear aromatic rings that have alkyl side chains and incorporate heteroatoms (such as O, N and S). The heteroatomic polar functional groups confer a limited molecular solubility of asphaltenes in hydrocarbon solvents that are partially or fully aliphatic. In organic solvents, asphaltenes associate to form discoidal aggregates 3–15 nm in diameter. In petroleum, these aggregates are solvated by resins. Oxygen and nitrogen functional groups are likely the major cause of the

<sup>†</sup> Presented at the 5th International Conference on Petroleum Phase Behavior and Fouling.

\* Author to whom correspondence should be addressed. Telephone: (919) 515-7121. E-mail address: peter-k@eos.ncsu.edu.

<sup>‡</sup> Current address: Champion Technologies, 2300 Premier Way, Sherwood Park, AB, T8H 2L2, Canada.

(1) Mansoori, G. A. Deposition and Fouling of Heavy Organic Oils and Other Compounds. In *Proceedings of the 9th International Conference on Properties and Phase Equilibria for Product and Process Design*, Kurashiki, Okayama, Japan, May 20–25, 2001. (Invited paper.)

(2) Misra, S.; Baruah, S.; Singh, K. Paraffin Problems in Crude Oil Production and Transportation: A Review. *SPE Prod. Facil.* **1995**, (February), 50–54.

(3) Thawer, R.; Nicoll, D. C. A.; Dick, G. Asphaltene Deposition in Production Facilities. *SPE Prod. Facil.* **1990**, (November), 475–480.

(4) Rassamdana, H.; Dabir, B.; Nematy, M.; Farhani, M.; Sahimi, M. Asphalt Flocculation and Deposition: I. The Onset of Precipitation. *AIChE J.* **1996**, *42*, 10–22.

(5) Rassamdana, H.; Sahimi, M. Asphalt Flocculation and Deposition: II. Formation and Growth of Fractal Aggregates. *AIChE J.* **1996**, *42*, 3318–3332.

(6) Agrawal, K. M.; Khan, H. U.; Surianarayanan, M.; Joshi, G. C. Waxy-deposition of Bombay High Crude Oil under Flowing Conditions. *Fuel* **1990**, *69*, 794–796.

(7) Nelson, W. L. *Petroleum Refinery Engineering*; McGraw-Hill: New York, 1958.

(8) Pfeiffer, J. P.; Saal, R. N. J. Asphaltic Bitumen as Colloid System. *J. Phys. Chem.* **1940**, *44*, 139–149.

interfacial activity of asphaltenes. These polar moieties, along with p-bonding among aromatic moieties, are also probably responsible for the aggregation of asphaltenes.<sup>9–12</sup>

During the recovery and transportation of petroleum, asphaltenes or waxes can precipitate when the thermodynamic stability of the colloidal solution is perturbed by changes in pressure, temperature, and/or composition.<sup>13–33</sup> A key unresolved issue is whether these two

classes of compounds interact synergistically in that precipitation process, i.e., whether the intermolecular interactions of some subset of the wax molecules with the precipitating asphaltene molecules (or vice versa) induces coprecipitation. If this were indeed the case, one would expect both the precipitated asphaltenes and waxes to differ significantly in chemical and physical properties from the corresponding asphaltenes and waxes in the parent crude oil.

Despite many years of research that has been focused on waxes and asphaltene precipitation,<sup>18–33</sup> there is still neither a consensus nor a fundamental understanding of the chemical identity of the solids that precipitate and deposit nor of the molecular species initially responsible for the phase change. Much of this uncertainty is attributable to the complex character—chemically and physically—of the asphaltenes and waxes.<sup>34–39</sup> What is intriguing about this complexity is that these two fractions probably differ the most in chemical and colloidal properties of all crude fractions: i.e., asphaltenes are the most aromatic and polar fraction and waxes are the most aliphatic and nonpolar fraction. Despite these strong chemical differences, these two fractions are similar in that both can be very high in molecular weight, both can aggregate or associate in solution, and both have marginal solubilities in crude oil. Thus, both are frequently involved in organic solid precipitation and deposition.<sup>1,2</sup> Yet, understanding the chemistry of precipitation and deposition is important both for economic and environmental reasons.

This paper describes, in a detailed chemical and physical fashion, the asphaltene and wax fractions of a series of parent crude oils and the organic deposits that have precipitated and have been isolated from these crudes as solid deposits. In addition, we attempt to resolve the issue of synergistic coprecipitation of waxes and asphaltenes. Based on what we present here, we conclude that waxes and asphaltenes *do not* interact molecularly to yield a synergistic coprecipitate; rather, one species precipitates because a thermodynamic solid–liquid phase boundary is crossed and the other species becomes entrained in the precipitating solid.

Waxes, asphaltenes, resins, and inorganic solids were isolated from five crude oils and the five corresponding organic deposits were subjected to detailed chemical analysis—including elemental analysis, Fourier transform infrared (FTIR) spectroscopy, <sup>1</sup>H and <sup>13</sup>C nuclear magnetic resonance (NMR) spectroscopy, high-temperature simulated distillation, and vapor pressure os-

(9) Moschopedis, S. E.; Speight, J. G. Investigation of hydrogen bonding by oxygen functions in Athabasca bitumen. *Fuel* **1976**, *55*, 187–192.

(10) Ignasiak, T.; Strausz, O. P.; Montgomery, D. S. Oxygen distribution and hydrogen bonding in Athabasca asphaltene. *Fuel* **1977**, *56*, 359–365.

(11) Acevedo, S.; Mendez, B.; Rojas, A.; Layrissr, L.; Rivas, H. Asphaltenes and Resins from the Orinoco Basin. *Fuel* **1985**, *64* (12), 1741–1748.

(12) Kilpatrick, P. K.; Spiecker, P. M. Asphaltene Emulsions. In *Encyclopedic Handbook of Emulsion Technology*; Sjoblom, J., Ed.; Marcel Dekker: New York, 2001; Vol. 3, pp 707–730.

(13) Monger, T. G.; Fu, J. C. The nature of CO<sub>2</sub>-induced Organic Deposition. Presented at the SPE Annual Technology Conference and Exhibition, Dallas, TX, September 27–30, 1987, SPE Paper No. 16713.

(14) Hirschberg, A.; deJong, L. N. J.; Schipper, B. A.; Meijer, J. G. Influence of Temperature and Pressure on Asphaltene Flocculation. *Soc. Pet. Eng. J.* **1984**, (6), 283–293.

(15) Sheu, E. Y.; Tar, M. M. De; Strom, D. A. Structure and Interaction of Asphaltene Colloids in Organic Solvents. In *Asphaltene Particles in Fossil Fuel Exploration, Recovery, Refining, and Production Processes*; Sharma, M. K., Yen, T. F., Eds.; Plenum Press: New York, 1994.

(16) Sheu, E. Y.; Storm, D. A. Colloidal Properties of Asphaltenes in Organic Solvents. In *Asphaltenes: Fundamentals and Applications*; Sheu, E. Y., Mullins, O. C., Eds.; Plenum Press: New York, 1995; pp 1–52, 115–143.

(17) Sheu, E. Y. Self-Association of Asphaltenes: Structure and Molecular Parking. In *Structures and Dynamics of Asphaltene*; Mullins, O. C., Sheu, E. Y., Eds.; 1998, Plenum Press: New York; pp 115–143.

(18) Park, S. J.; Mansoori, G. A. Aggregation and Deposition of Heavy Organics in Petroleum Crudes. *Energy Source* **1988**, *10*, 109–125.

(19) Hansen, J. H.; Fredenslund, A.; Pedersen, K. S.; Ronningsen, H. P. A thermodynamic Model for Predicting Wax Formation in Crude Oils. *AIChE J.* **1988**, *34* (12), 1937–1942.

(20) Fuhr, B. J.; Cathrea, C.; Coates, L.; Kalra, H.; Majeed, A. I. Properties of Asphaltenes from a waxes crude. *Fuel* **1991**, *70*, 1293–1297.

(21) Chung, F.; Sarathi, P.; Jones, R. Modelling of Asphaltene and Wax Precipitation, U. S. Department of Energy Report No. NIPER-498 (DE 91002217), January 1991.

(22) Chung, T. H. Thermodynamic Modelling for Organic Solid Deposition. U.S. Department of Energy Report No. NIPER-623 (DE 93000104), December 1992.

(23) Boer, R. B.; Leerlooyer, K.; Eigner, M. R. P.; van Bergen, A. R. D. Screening of Crude Oils for Asphalt Precipitation: Theory, Practice, and the Selection of Inhibitors. *SPE Prod. Facil.* **1995**, (2), 55–61.

(24) Thomas, D. C.; Becker, H. L.; Del Real Soria, R. A. Control Asphaltene Deposition in Oil Wells. *SPE Prod. Facil.* **1995**, (5), 119–123.

(25) Ferworn, K. A. Thermodynamic and Kinetic Modelling of Asphaltene Precipitation From Heavy Oils and Bitumens, Ph.D. Thesis, The University of Calgary, Calgary, Alberta, Canada, April 1995.

(26) Mansoori, G. A.; Jiang, T. S.; Kawanaka, S. Asphaltene deposition and its role in petroleum production and processing. *Arabian J. Sci. Eng.* **1988**, *13* (1), 17.

(27) Mansoori, G. A. Modeling of Asphaltene and other heavy organic deposition. *J. Pet. Sci. Eng.* **1997**, *17*, 101–111.

(28) Buckley, J. S.; Hirasaki, G. J.; Drasek, S. V.; Wang, J.-X.; Gill, B. S. Asphaltene Precipitation and Solvent Properties of Crude oils. In *2nd International Symposium on Thermodynamics of Heavy Oils and Asphaltenes*, Session II, Spring National Meeting Houston, TX, March 9–13, 1997, 61f.

(29) Carbognani, L.; Duarte, D.; Rosales, J.; Villalobos, J. Isolation and characterization of Paraffinic components from Venezuelan asphalts. Effects of paraffin dopants on rheological properties of some asphalts. *Pet. Sci. Technol.* **1998**, *16* (9&10), 1085–1111.

(30) Carbognani, L.; Orea, M.; Fonseca, M. Complex Nature of Separated Solid Phases from Crude Oils. *Energy Fuels* **1999**, *13*, 351–358.

(31) Carbognani, L.; DeLima, L.; Orea, M.; Ehrmann, U. Studies on Large Crude Oil Alkanes: II. Isolation and characterization of Aromatic Waxes and Waxy asphaltenes. *Pet. Sci. Technol.* **2000**, *18* (5&6), 607–634.

(32) Garcia, M. d. C. Crude Oil Wax Crystallization. The Effect of Heavy *n*-paraffins and Flocculated Asphaltenes, *Energy Fuels* **2000**, *14*, 1043–1048.

(33) Bennett, H. *Industrial Waxes, Part 1: Natural Waxes*; Chemical Publishing Company: New York, 1963; p 1.

(34) Musser, J. B.; Kilpatrick, P. K. Molecular Characterization of Wax Isolated from a Variety of Crude Oils. *Energy Fuels* **1998**, *12* (4), 715–725.

(35) Dickie, J. P.; Yen, T. F. Macrostructures of the Asphaltic Fractions by Various Instrumental Methods. *Anal. Chem.* **1967**, *39* (14), 1847–1852.

(36) Yen, T. F. Structure of Petroleum Asphaltene and its Significance. *Energy Sources* **1974**, *1* (4), 447–463.

(37) Speight, J. G. Latest Thoughts on the Molecular Nature of Petroleum Asphaltenes. *Prepr. Pap.-Am. Chem. Soc., Div. Pet. Chem.* **1989**, *34* (2), 321–328.

(38) Rogel, E. Simulation of Interactions in Asphaltene Aggregates. *Energy Fuels* **2000**, *14*, 566–574.

(39) McLean, J. D.; Kilpatrick, P. K. Effects of Asphaltene Aggregation in Model Heptane–Toluene Mixtures on Stability of Water-in-Oil Emulsions. *J. Colloid Interface Sci.* **1997**, *196*, 23–34.

**Table 1. Crude Oil and Deposit Source and Designation**

sample	symbol used in this paper	resource
Crude Oil		
crude A	A	Gannet
crude B	B	GOM
crude C	C	Beta
crude D	D	Fulmar
crude E	E	Venezuela
Deposit		
deposit A	δA	Gannet, no description
deposit B	δB	GOM, associated pigged pipeline deposit
deposit C	δC	Beta, pipeline deposit
deposit D	δD	Fulmar, separator deposit
deposit E	δE	Venezuela, asphaltenic deposit
deposit F	δF	GOM, associated pigged pipeline deposit

mometry (VPO). In addition, a sixth deposit was also studied. Elemental analysis provides structural information regarding relative aromatic (H/C ratio) and heteroatomic distribution (N, S, and O percentages) in the waxes, asphaltenes, crude oils, and deposits. The presence of functional moieties—including carbonyls/carboxylic acids, phenols, sulfonyls, amide carbonyls, and pyrroles and the aromatic carbon content in these polar fractions—were evaluated by means of FTIR spectroscopy. The straight-chain methylene content in the waxes was semiquantified by the rocking-mode vibration at 720–730  $\text{cm}^{-1}$ . Proton and  $^{13}\text{C}$  NMR spectroscopy were used to provide structural information on aliphatic and aromatic hydrocarbon groups in waxes. Based on these results, the chemistry of waxes and asphaltenes from the original crude oils and their corresponding deposits were compared and contrasted. In addition, differential solubility tests and VPO measurements were performed to probe the chemistry of the asphaltenes by dissolving them in mixtures of heptane and toluene, varying the aliphatic–aromatic balance of the mixtures and monitoring the saturation solubility and the precipitation percentage of the asphaltene fractions.

## 2. Experimental Section

**2.1. Materials.** Five crude oils (designated as A, B, D, C, and E), five corresponding deposits (designated as δA, δB, δD, δC, and δE), and another deposit (denoted as δF) were collected and supplied by Shell International E&P TAR and Equilon. Table 1 lists the sources of these crudes oils and deposits.

*n*-Heptane, toluene, methylene chloride, petroleum ether, cyclohexanes, and acetone (all high-performance liquid chromatography (HPLC) grade) were acquired from Fisher Scientific. Petroleum ether was optimum grade. The silica gel was from Fisher Scientific (chromatographic grade, 35–60 mesh, Davisil). The filter paper used for isolating crude asphaltenes was Whatman 934 AH glass microfiber filter. For isolating wax, the filter paper was 542 hardened ashless filter paper (pore size of 2.7  $\mu\text{m}$ ).

**2.2. Procedures for Isolating Asphaltenes, Waxes, and Inorganic Fractions from Crude Oils and Their Corresponding Deposits.** Asphaltenes, saturates, aromatics, and resins were separated from crude oils by the IP 143 standard. The asphaltenes were precipitated by heptane, and resins were obtained by sequential elution chromatography of maltenes adsorbed to silica gel. The asphaltenes from deposits were separated by a modified IP 143 procedure (provided by Shell Oil Company). A schematic of the separation procedure is shown in Figure 1.

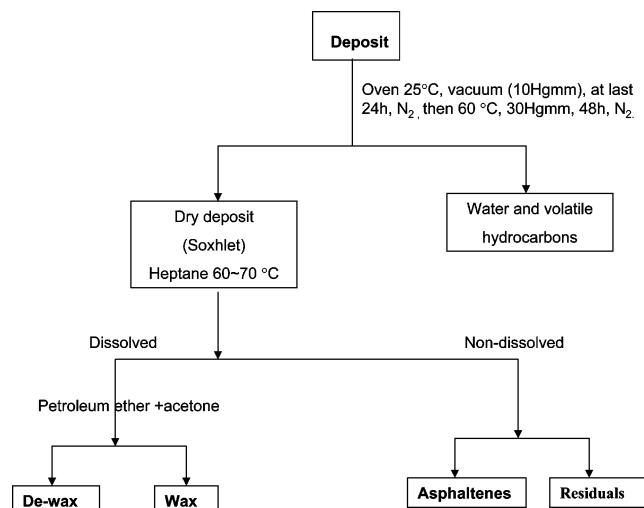


**Figure 1.** Schematic illustration of method for separating fractions from deposits.

Wax fractions in the crude oils were isolated from the saturated hydrocarbon fractions. using a method proposed by Burger in 1981<sup>40</sup> and subsequently modified by other researchers.<sup>34</sup> Five grams of saturates from crude oils were dissolved in 35 mL of petroleum ether, and then 105 mL of acetone were added. Saturates, petroleum ether, and acetone mixtures, all of the filtration apparatus, and a wash solvent composed of acetone and petroleum ether (3:1 v/v) were cooled for 2 h at  $-20\text{ }^{\circ}\text{C}$ . The mixture was filtered through a Buchner funnel into a 100-mL flask and a vacuum was applied. The retentate was washed with cold wash solvent until clear solvent flowed. The retentate was transferred to a tared vial and dried in a nitrogen-flushed vacuum oven at  $60\text{ }^{\circ}\text{C}$  for 48 h.

Asphaltenes and maltenes were obtained from deposits by the modified IP 143 method. The deposits were extracted at a 1:40 hot heptane ( $70\text{ }^{\circ}\text{C}$ ) ratio in a Soxhlet extractor for a minimum of 12 h. Heptane was removed in a rotary evaporator, and the residual maltenes were obtained. After extraction of maltenes, asphaltenes were then extracted from deposits with a 10-fold excess of methylene chloride. Methylene chloride was removed in a rotary evaporator from the asphaltene solution. Residual maltenes and the asphaltene were dried in a nitrogen-flushed vacuum oven at  $60\text{ }^{\circ}\text{C}$  for 48 h. Wax fractions were obtained from the maltenes separated using Soxhlet extraction. A mixture of petroleum ether and acetone (1:3 v/v) was added in 7-fold excess to the maltenes. The subsequent wax precipitation method was the same as that used to isolate waxes from the crude.

**2.3. Elemental Analysis.** Elemental analysis (carbon, hydrogen, nitrogen, sulfur, and oxygen) of crude oils, deposits, waxes, asphaltenes, and metals analysis of asphaltenes were performed by Galbraith Laboratories, Inc. A combustion method was used to determine the carbon, hydrogen, nitrogen, and sulfur content to within  $\pm 0.55\%$ , according to the methodologies described in ASTM D5373 and ASTM D5291. The samples were pyrolyzed in a helium/hydrogen mixture to determine the oxygen content.

**2.4. High-Temperature Simulated Distillation (HTSD).** High-temperature simulated distillation (HTSD)<sup>41</sup> is a relatively new method that extends ASTM Method D 2887 (IP 4060) for the determination of the boiling range distribution

(40) Burger, E. D.; Perkins, T. K.; Striegler, J. H. Studies of Waxy-deposition in the Trans Alaska Pipeline. *J. Pet. Technol.* **1981**, 1075–1086.

(41) Villalanti, D.; Janson, D.; Colle, P. Distillation Session, Distillation Column Design and Operation-IV: Advances in Distillation Modeling and Simulations. Presented at the AIChE Spring National Meeting, Houston, TX.; March 1995; pp 19–23. (Paper No. B (preprint).)

**Table 2. Elemental Compositions and Properties of Crude Oils and Their Deposits**

	H/C	C (%)	H (%)	N (%)	S (%)	O (%)	asphaltene (%)	wax (%)	API gravity	type of crude oil
crude oil										
A	1.85	86.32	13.26	<0.5	0.15	0.86	0.1	11.6	41.5	light
B	1.82	86.22	13.03	<0.5	0.2	1.17	NM <sup>a</sup>	2.7	34.6	light
C	1.66	82.74	11.47	0.81	3.69	1.27	12.1	4.2	15.5	heavy
D	1.90	85.78	13.54	<0.5	<0.5	<0.5	0.6	8.0	39.0	light
E	1.79	84.77	12.45	<0.5	1.89	0.76	6.5	2.8	25.9	heavy
	H/C	C	H	N	S	O	asphaltene (%)	wax (%)	inorganic + solid (%)	type of deposit
deposit										
δA	2.03	83.01	13.9	<0.5	<0.5	1.02	0.2	75.7	0.8	wax
δB	1.88	84.19	13.19	<0.5	0.18	1.82	NM <sup>a</sup>	43.7	1.5	
δC	1.88	83.46	13.06	<0.5	1.98	1.49	6.1	55.7	2.8	
δD	0.91	86.82	9.12	<0.5	1.25	1.55	55.7	4.0	NM <sup>a</sup>	asphaltenic
δE	1.48	81.11	10.02	0.73	4.01	2.51	27.4	4.3	7.0	
δF	2.05	62.81	10.74	2.13	0.28	19.66	63.6	1.8		neither asphaltenic nor wax

<sup>a</sup> Not measured.**Table 3. Weight Percentages of SARA Fractions of Crude Oils**

fraction	sample A	sample B	sample C	sample D	sample E
nonvolatile saturates + aromatics + resins (%)	49.9	76.4	77.6	67.8	70.2
wax (%)	11.6	2.7	4.2	8.0	2.8
asphaltenes (%)	0.1	NM	12.1	0.6	6.5
water (%)	0.04	0.06	0.21	0.70	0.71
pretreatment volatiles (%)	38.5	20.8	6.0	23.5	19.8

**Table 4. Weight Percentages of SARA Fractions of Deposits**

fraction	sample δA	sample δB	sample δC	sample δD	sample δE	sample δF
saturates + aromatics + resin (%)	10.3	34.5	27.6	35.1	40.6	11.3
wax (%)	75.7	43.7	55.7	4.0	4.3	63.6 <sup>a</sup>
asphaltene (%)	0.2	NM	6.1	55.7	27.4	
inorganic + solid (%)	0.8	1.5	2.8	NM	7.0	1.8
pretreatment volatiles (%)	10.9	19.6	7.2	5.07	16.2	19.9
water (%)	2.12	0.85	0.58	0.13	4.1	3.4
entrained oil/wax + asphaltene (%)	27.9	123.7	54.2	67.38	179.0	49.0

<sup>a</sup> Neither asphaltene nor wax; see Table 15 for a detailed description.

of hydrocarbons up to a final boiling point of 760 °C. Recent advances in capillary gas chromatography (GC) columns and stationary phases, together with programmed temperature vaporization (PTV) and on-column injection techniques, enable separation of C<sub>5</sub>–C<sub>120</sub> normal paraffins and permits characterization of petroleum products from 36.1 °C to 748.9 °C. Triton Analytic Corporation provided the HTSD analysis. The boiling range distributions of hydrocarbons in the crude oils, deposits, and waxes were all determined using this technique.

**2.5. Measurement of Wax Melting Region.** The temperature range of melting and the optical textures of phases of the crude and deposit waxes were observed using an Olympus BH-2 polarizing microscope that was equipped with a Physitemp TS-4ER temperature-controlled hot stage (–20 °C to 100 °C). The temperatures corresponding to the initial melting of wax crystals until all of the visible wax crystals disappeared was observed and reported as the melting range. Waxes were first heated to 35 °C and maintained at this temperature for 5 min to determine if wax crystals had begun to melt. The temperature was then increased by an additional increment of 5 °C for each 5 min interval. This step was repeated until all of the wax crystals completely melted. Because waxes were a mixture of hydrocarbon compounds, some deposit waxes melted over a large region with an uncertainty of ±5 °C.

**2.6. Fourier Transform Infrared Spectroscopy.** An RFX-65 spectrometer that was equipped with a liquid nitrogen-cooled mercury cadmium telluride (MCT) detector was used to obtain FTIR spectra of asphaltene and wax solutions. Cyclohexane was used to dissolve the waxes (5–15 g/L), and spectra were obtained in a KCl cell with a 0.25-mm spacer. Methylene chloride was used to dissolve the asphaltenes (5–15 g/L), and spectra were obtained in a CaF<sub>2</sub> cell with a 0.2008-mm spacer. Background spectra of pure cyclohexane or methylene chloride were integrated and subtracted from sample spectra. Two

hundred fifty-six scans were taken of each sample recorded from 4000 cm<sup>–1</sup> to 400 cm<sup>–1</sup> at a resolution of 4 cm<sup>–1</sup>. Peak positions and areas were determined using available software packages. Areas under absorption bands of interest were converted to functional group concentrations via Beer's law.

**2.7. Solubilities of Asphaltenes in Toluene–Heptane Mixtures with Different Ratio.** A series of various concentrations (0.001%–0.008%, w/w) of asphaltene–toluene solutions were prepared, and their ultraviolet (UV)–visible spectra were obtained in the wavelength range of 200–800 nm, using a Shimadzu UV–Vis scanning spectrophotometer. The absorbance at 450 nm was used to obtain asphaltene concentrations, being sufficiently high to be uninfluenced by the Soret band or by any modest attenuation of light, because of scattering of any residual undissolved material. The absorbance range was 0.2–1.2. Toluene–heptane (T/H) mixtures of various volume proportions were prepared, to which asphaltenes were added. These solutions/dispersions were shaken for more than 48 h to ensure saturation. The asphaltene solutions were filtered through a 1.6-μm filtering syringe tip; the saturated filtrate solutions were weighed and dried under N<sub>2</sub> gas, and the dried asphaltenes were redissolved in toluene as accurate concentrations to measure their UV–visible spectra and to obtain the saturation concentration. The saturation concentrations of asphaltene in different T/H mixtures were obtained by means of their absorbance in the 450-nm wavelength and the corresponding calibration.

### 3. Results and Discussion

**3.1. Categorizing Crude and Deposits.** The properties and compositions of the five parent crude oils (A–E) and their corresponding deposits (δA–δE) are listed in

**Table 5. Weight Percentages of HTSD Fractions in Whole Crude Oils and Deposits**

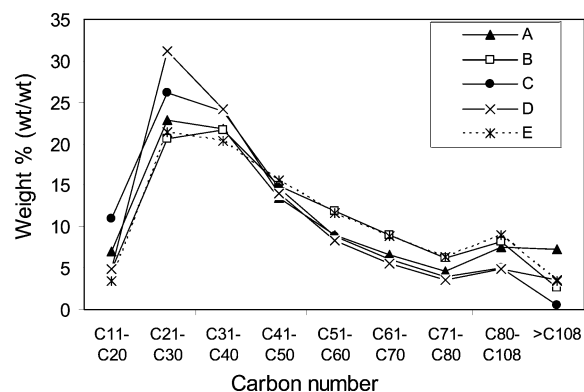
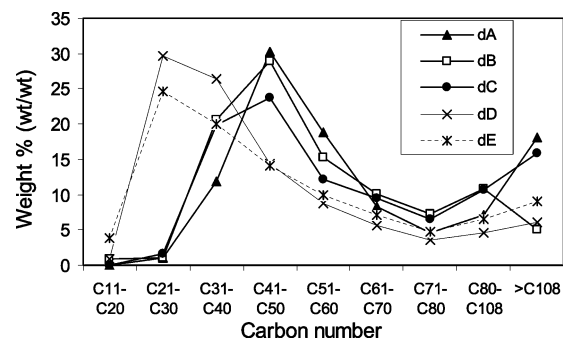
sample	HTSD Fraction (wt %)			sum
	<350 °C	350–550 °C	>550 °C	
Crude Oils				
A	97.0	2.1	0.4	99.5
B	98.0	1.5		99.5
C	47.6	33.1	9.6	90.3
D	97.1	2.0	0.4	99.5
E	72.5	15.1	4.4	92.0
Deposits				
δA	5.1	20.7	25.8	51.6
δB	69.4	18.6	4.7	92.7
δC	5.2	55.4	19.6	80.2
δD	23.5	27.3	4.3	55.1
δE	17.2	39.4	9.1	65.7

**Table 6. Melting Ranges of Crude Oil Waxes and Associated Deposit Waxes**

wax	H/C ratio	appearance	melting range (°C)
Crude Oil			
A	1.94	white yellow	50–53
B	2.00	yellow	45–75
C	1.85	orange	40–45
D	2.01	white yellow	60–65
E	1.95	white yellow	40–50
Deposit			
δA	2.00	brown, solid	75–95
δB	1.96	brown, solid	85–95
δC	1.92	brown, solid	85–95
δD	1.96	orange	55–85
δE	1.89	yellow	40–50

Tables 2–4. Crude oils A and B contain virtually no asphaltenes, whereas crude oil D contains a low concentration of asphaltenes (0.55% w/w). The HTSD results of crude oils A, B, and D indicated that their fractions with a boiling point of  $\leq 350$  °C were close to 100% (97%–98%; see Table 5). The API of these three crude oils was  $>35$ , indicating that these are light, paraffinic crudes. Crude oils C and E contain higher asphaltene amounts (6%–12%, w/w). The HTSD results of crude oils C and E showed that 20%–40% of these crudes boils at  $>350$  °C and there was still ca. 10% that did not distill, even at temperatures of  $>550$  °C. Their API gravities were 12 and 25 respectively, corresponding to relatively heavy asphaltenic crudes.

Table 3 presents wax or asphaltene contents in the deposits, which are clearly higher than other constituents (e.g., occluded oil, water, inorganic materials). The deposits fall into two groups: waxy deposits and asphaltenic deposits (see Table 2). The wax contents in deposits δA, δB, and δC are  $>40$  wt %, and these samples are classified as waxy deposits. The asphaltene contents in δD and δE are  $>27$  wt %, and they are therefore classified as asphaltenic deposits. With both waxy deposits and asphaltenic deposits, 10%–120% hydrocarbons coprecipitated with them to form organic deposits. A comparison of the properties of waxy deposits to those of their parent oils shows that the H/C ratios of waxy deposits are greater than the H/C ratios of the parent crude oils, indicative of a greater degree of paraffinic aliphaticity in the deposits. Conversely, the H/C ratios of asphaltenic deposits were much less than the H/C ratios of their parent crude oils. Tables 3 and 4 show the relatively low content of maltenes (saturates, aromatics, and resins) in deposits, in comparison to their parent crude oils. Their elemental analyses showed that the oxygen content clearly increased in deposits, indicating perhaps the origin of reduced solubility or

**Figure 2.** Carbon number distribution of crude oil waxes from flame ionization detection (FID) response in high-temperature simulated distillation (HTSD) analysis.**Figure 3.** Carbon number distribution of deposit waxes from FID response in HTSD analysis.

increased tendency to precipitate and adsorb. The fraction of material with boiling points of  $<350$  °C in the deposits was much smaller than that in the crude oils (see Table 5), whereas the fractions of the material with boiling points in the range of 350–550 °C were increased significantly, compared to the parent crude oils. The fractions with a boiling point of  $>550$  °C were also expected to be a higher percentage of the deposits than in the parent crude oils. HTSD yields for deposits were much lower than their corresponding crudes. It is easy to understand the low yields for deposits δC and δD, because of the relatively high concentration of asphaltenes in them. With deposit δA, the yield of HTSD was ca. 50%, much lower than that of deposit δB, both of which have low asphaltene contents. Plausible explanations for the lower HTSD yields are that some of the δA fraction could not be totally dissolved in CS<sub>2</sub> or that there are higher carbon number species that cannot elute from the column.

Regarding the appearance of the waxy deposits, deposit δA is a brown sandy solid, whereas deposits δB and δC are dark brown and greasy in appearance. Almost no asphaltenes could be measured in deposits δA and δB, whereas in deposit δC, 6% asphaltenes coprecipitated with the wax.

The asphaltenic deposits had a markedly different appearance. Two forms of asphaltenic deposits are observed in the field:<sup>42</sup> hard, shiny, solid deposits and dark sludge. The appearance of deposit δD was the former, whereas that of deposit δE seemed to be the

(42) Leontaritis, K. J.; Amaefule, J. O.; Charles, R. E. A Systemic Approach for the Prevention and Treatment of Formation Damage Caused by Asphaltene Deposition. *SPE Prod. Facil.* **1994**, (August), 157.

**Table 7. Properties of Crude Oil Waxes and Associated Deposit Waxes (a) in Wax Deposits and (b) in Asphaltenic Deposits**

sample	weight in sample (%)	H/C ratio	S/C ratio	O/C ratio	C (%)	H (%)	S (%)	O (%)	sum (%)	appearance
(a) Wax Deposits										
A	8.14	1.94	0.0003	0.0048	85.34	13.78	0.057	0.54	99.72	white yellow
$\delta$ A	75.7	2.00			85.25	14.14			99.39	tan, light brown
B	1.59	2.00		0.0168	86.03	14.35	<0.16	1.93	102.31	white yellow
$\delta$ B	43.6	1.96		0.009	84.41	13.8	<0.32	1.01	99.39	tan, light brown
C	3.48	1.85	0.0062	0.0085	84.92	13.09	1.4	0.96	99.83	yellow
$\delta$ C	55.72	1.92	0.0046	0.0087	84.3	13.51	1.04	0.98	100.37	tan, light brown
(b) Asphaltenic Deposits										
D	7.97	2.01			85.67	14.37	<0.1	<0.5	100.04	white yellow
$\delta$ D	3.95	1.96			85.18	13.87	<0.5	<0.5	99.05	yellow
E	2.80	1.95	0.0021		85.21	13.81	0.47	<0.5	99.99	white yellow
$\delta$ E	4.33	1.89	0.0035	0.006	85.71	13.52	0.81	0.68	100.72	yellow

**Table 8. Fourier Transform Infrared (FTIR) Absorbance Maxima of Straight-Chain Alkanes at 735–700  $\text{cm}^{-1}$ <sup>a</sup>**

compound	molecular formula	number of $-(\text{CH}_2)-$ units <sup>b</sup>	absorbance peak ( $\text{cm}^{-1}$ )	$-(\text{CH}_2)_4-$ in entire molecule (wt %)
<i>n</i> -pentane	$\text{C}_5\text{H}_{12}$	3	732	
<i>n</i> -hexane	$\text{C}_6\text{H}_{14}$	4	726	65.12
<i>n</i> -heptane	$\text{C}_7\text{H}_{16}$	5	723	70.00
<i>n</i> -decane	$\text{C}_{10}\text{H}_{22}$	8	721	78.87
2,6-dimethyloctane	$\text{C}_{10}\text{H}_{22}$	3	734	
3,3-dimethyloctane	$\text{C}_{10}\text{H}_{22}$	4	725	39.44
2,2-dimethyloctane	$\text{C}_{10}\text{H}_{22}$	5	724	49.29
5-methylnonane	$\text{C}_{10}\text{H}_{22}$	3	729	
4-methylnonane	$\text{C}_{10}\text{H}_{22}$	4	725	39.44
3-methylnonane	$\text{C}_{10}\text{H}_{22}$	5	724	49.29
2-methylnonane	$\text{C}_{10}\text{H}_{22}$	6	723	59.15
<i>n</i> -dodecane	$\text{C}_{12}\text{H}_{26}$	10	721	82.35
<i>n</i> -hexadecane	$\text{C}_{16}\text{H}_{34}$	14	721	86.73
octadecane	$\text{C}_{18}\text{H}_{38}$	16	718	88.19
nonadecane	$\text{C}_{19}\text{H}_{40}$	17	720	88.81
2,6,10,14-tetramethyl pentadecane	$\text{C}_{19}\text{H}_{40}$	3	736	
<i>n</i> -triacontane	$\text{C}_{30}\text{H}_{62}$	28	720	92.89
<i>n</i> -tetracontane	$\text{C}_{40}\text{H}_{82}$	38	720	94.66

<sup>a</sup> The data were arranged based on ref 44. <sup>b</sup> The number of connected methylene functional groups in the molecule.

latter. Based on the considerably higher amount of asphaltenes in deposit  $\delta$ D compared to deposit  $\delta$ E (55.7% vs 27.4%), and considering the polar, high-molecular-weight, highly aromatic character of  $\delta$ D asphaltenes, this is not surprising. In the following section, we focus our attention on comparing and contrasting the properties of waxes and asphaltenes that were isolated from both crude oils and their respective deposits.

**3.2. Wax Fraction Analyses.** Three categories of waxes—crude, waxy deposit, and asphaltenic deposit—were classified according to their sources. The ranges of melting, H/C ratios, and appearances of the three classes of waxes are listed in Table 6. The carbon number distributions of waxes are shown in Figures 2 and 3. Parts a and b of Table 7 compare the elemental distribution of crudes and their respective deposit waxes.

In FTIR spectra of long straight-chain alkanes, the peak at  $720 \text{ cm}^{-1}$ , as a finger peak, has long been associated with long, straight-chain methylene that is at least four units long.<sup>43</sup> Table 8 lists the absorbance peak location between 715 and  $735 \text{ cm}^{-1}$  in the FTIR spectra of straight-chain alkanes.<sup>44</sup> With *n*-alkanes ranging in carbon number from  $\text{C}_5$  to  $\text{C}_{44}$ , the absor-

bance peak exhibits a blue shift to ca.  $720 \text{ cm}^{-1}$  as the carbon number increases. 2,6,10,14-Tetramethylpentadecane, which is a  $\text{C}_{19}$  alkane with four methyl branches, had no vibrational mode at  $720 \text{ cm}^{-1}$  but does exhibit one at  $736 \text{ cm}^{-1}$ . Table 8 shows that, as the weight percentage of straight-chain methylene content increases in alkanes, the absorbance peak shifts closely to  $720 \text{ cm}^{-1}$ .

Figures 4 and 5 are FTIR spectra of all the waxes. The spectra clearly illustrate that (i) all crude and deposit waxes have significant peaks in the range  $720$ – $730 \text{ cm}^{-1}$  and (ii) these peaks in deposit wax are considerably more intense than those in their respective parent crude waxes. Table 9 lists the weight percentages of the straight-chain methylene contents in both crude and deposit waxes. The apparent integrated absorption intensities used to determine long, straight-chain methylene concentrations in this study was  $94.9 \text{ L mol}^{-1} \text{ cm}^{-1}$ .<sup>35</sup> Although the low molar apparent integrated absorption intensity could result in relatively large uncertainties in this measurement, the values in Table 9 are still plausible and provide useful clues about differences among waxes from crude versus organic deposits. The results in Table 9 show that deposit waxes contain more paraffinic waxes, with less apparent chain branching and cyclic character, than crude waxes.

**3.2.1. Properties and Compositions of Crude Waxes.** Most crude waxes melted in the range of  $40$ – $55 \text{ }^\circ\text{C}$ ; the D and B waxes had higher melting ranges ( $60$ – $65 \text{ }^\circ\text{C}$

(43) Bellamy, L. J. Alkanes. In *Advances in Infrared Group Frequencies: The Infrared Spectra of Complex Molecules*; Wiley: New York, 1964; Chapter 2.

(44) FTIR data from Spectral Database for Organic Compounds (SDBS), <http://www.aist.go.jp/RIODB/SDBS/menu-e.html>.

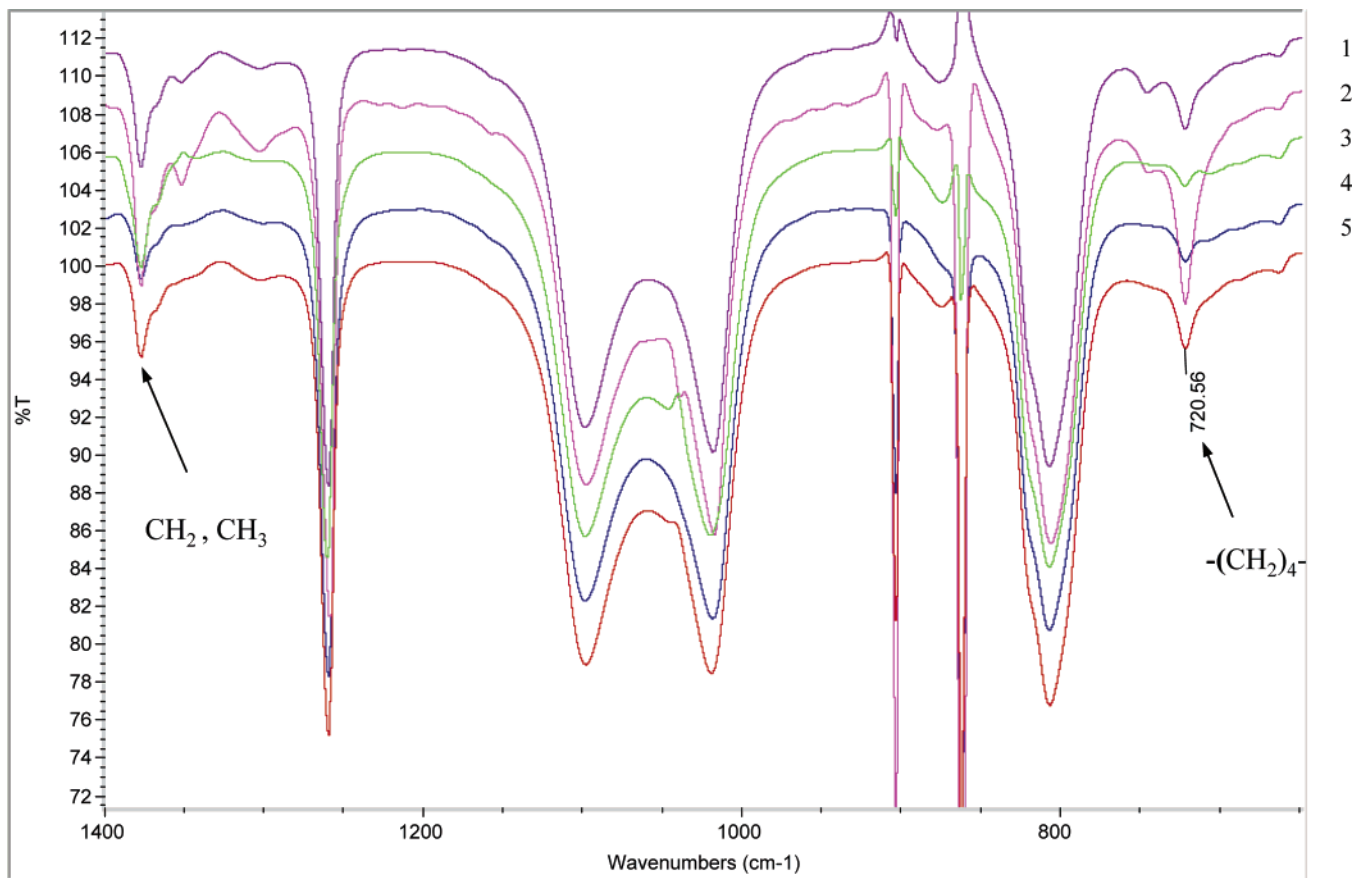


**Figure 4.** FTIR spectra of waxes isolated from crude oils: 1, E wax; 2, D wax; 3, B wax; 4, C wax; and 5, A wax.

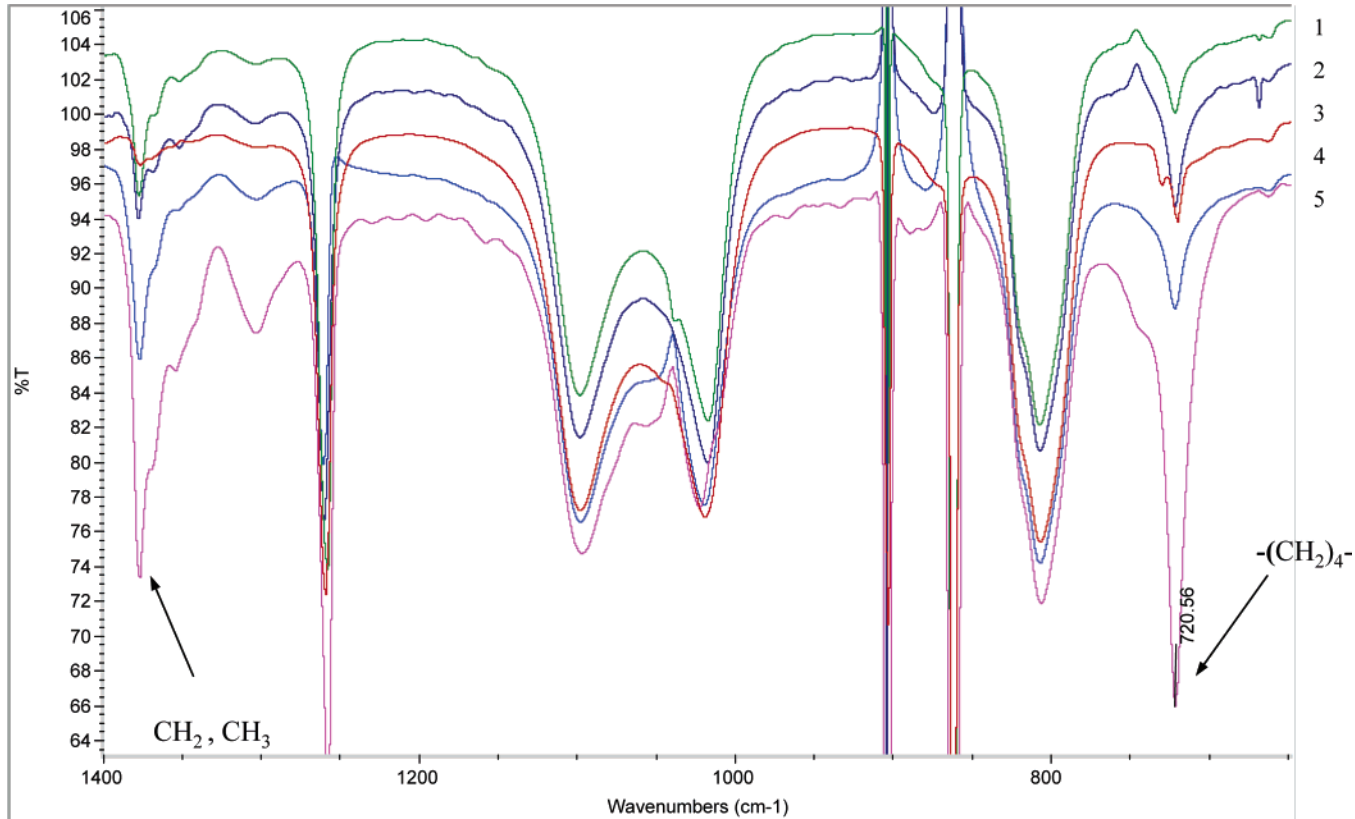


**Figure 5.** FTIR spectra of waxes isolated from deposits: 1,  $\delta$ E wax; 2,  $\delta$ D wax; 3,  $\delta$ C wax; 4,  $\delta$ B wax; and 5,  $\delta$ A wax.

and 45–75 °C, respectively; see Table 6). Microscopic observations show that there are fine crystalline structures in the D waxes, which may result in an increase

in the melting range.<sup>34</sup> B wax exhibited two melting regions (45–55 °C and 65–75 °C) and also contained part of a fine crystalline structure. The HTSD results

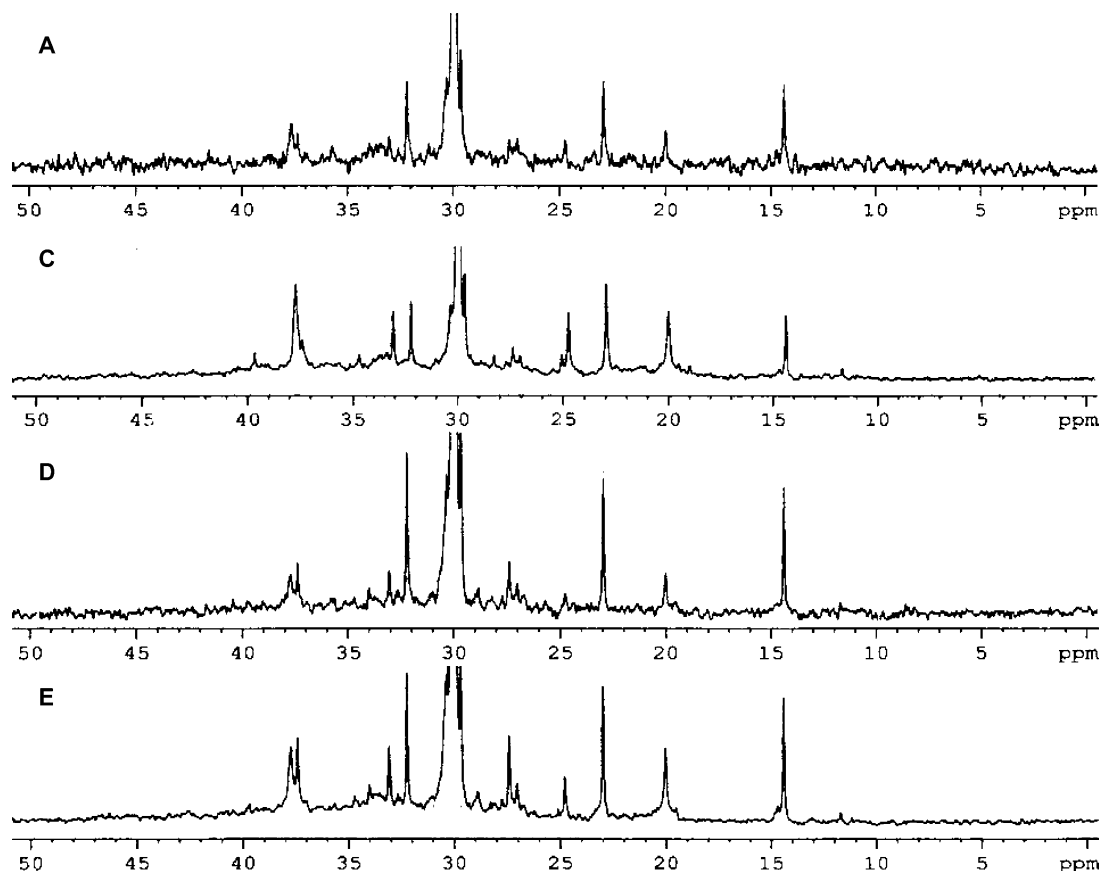


Figure 6.  $^{13}\text{C}$  NMR spectra of waxes isolated from crude oils.

Table 9. Weight Percentages of Straight-Chain Methylene in Waxes Based on FTIR Analysis

sample	$-(\text{CH}_2)_4-$ (wt %)	notes
		Crude Oils
A	63.8	} crude waxes
B	42.5	
C	18.8	
D	69.9	
E	48.6	
		Deposits
$\delta\text{A}$	80.5	} wax-deposit waxes
$\delta\text{B}$	66.5	
$\delta\text{C}$	40.3	
$\delta\text{D}$	80.9	} asphaltenic-deposit waxes
$\delta\text{E}$	59.3	

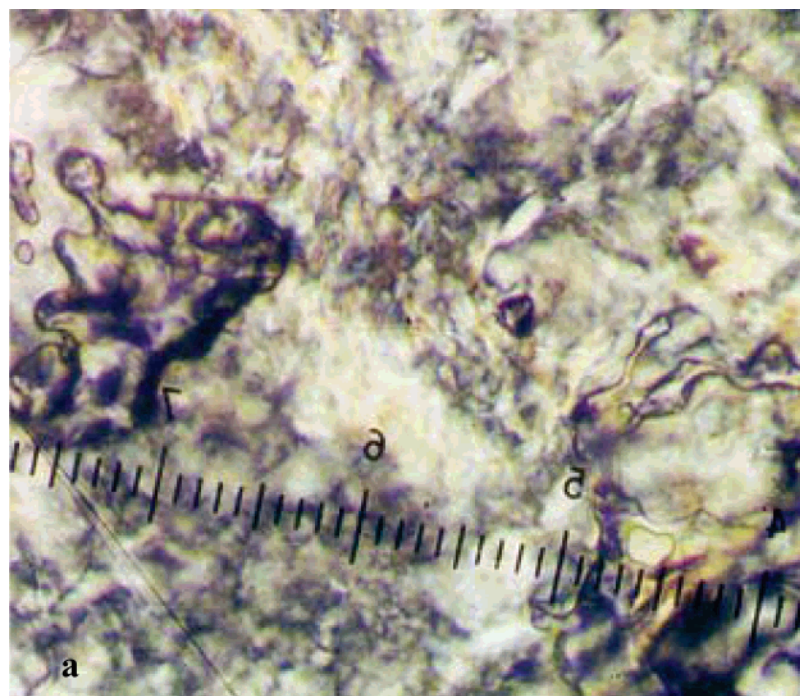
in Figure 2 suggest a very broad distribution of carbon numbers ( $\text{C}_{11}$ – $\text{C}_{108}$ ) in all crude waxes. The primary constituents were in the  $\text{C}_{20}$ – $\text{C}_{40}$  range (40%–55%), with other components being 5%  $\text{C}_{11}$ – $\text{C}_{20}$ , 15%  $\text{C}_{41}$ – $\text{C}_{50}$ , 5%–10%  $\text{C}_{51}$ – $\text{C}_{70}$ , and ca. 15%  $\text{C}_{>71}$  alkanes. Their elemental analyses indicate very low nitrogen (<0.1%) contents (see Table 7a and 7b). The sulfur and oxygen contents in crude waxes show some relationship to the content of sulfur and oxygen in their parent crude oils. The sulfur content in A, B and D waxes was <0.1%, and the parent crudes also have a very low sulfur content (see Table 2). Crude oils C and E contain a higher sulfur content, and their waxes also show a higher sulfur percentage (1.4% and 0.47%, respectively). The obviously lower H/C ratio of C wax is partially attributed to its higher sulfur content. Proton NMR spectra of crude waxes evidenced a small region of aromatic protons, although  $^{13}\text{C}$  NMR and FTIR spectra show that there were no measurable aromatic groups in the crude

waxes. The small amount of aromatic carbon present in the crude waxes could be present in thiophenic rings, as the literature reports.<sup>35</sup> From  $^{13}\text{C}$  NMR spectra (see Figure 6), most crude waxes exhibit methyl, methylene, methine, and quaternary carbon structures, indicative of considerable branching.

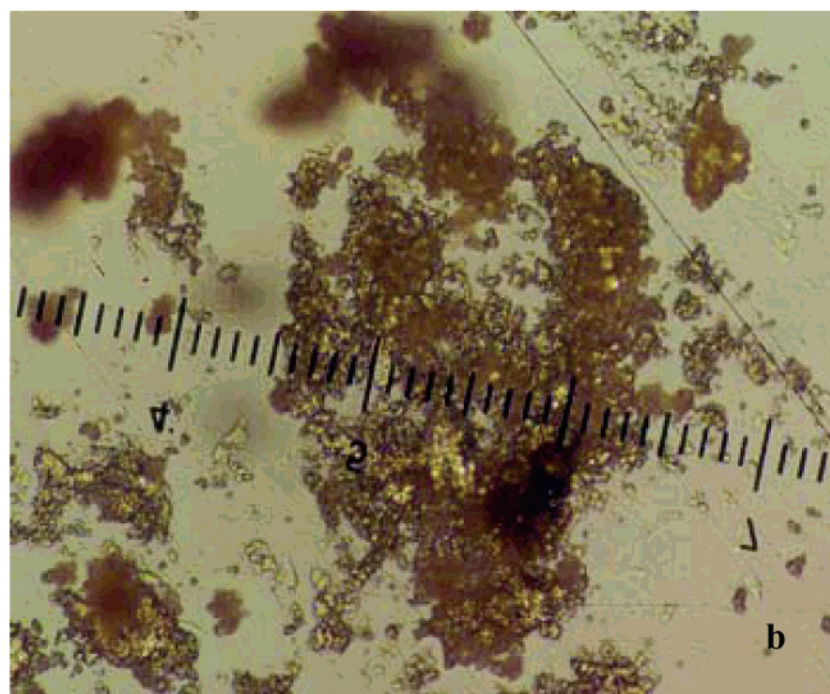
Based on the H/C ratios, melting points, and HTSD results, crude A, B, D, and E waxes are primarily paraffinic waxes; the C wax is a mixed paraffinic and fine crystalline wax with substantial chain branching and heteroatomic functionality.

**3.2.2. Properties and Compositions of Waxy-Deposit Waxes.** The waxes isolated from deposits  $\delta\text{A}$ ,  $\delta\text{B}$ , and  $\delta\text{C}$  as similar to clay in appearance. The melting points of these waxes fall in the range of 75–95 °C (see Table 6), which is much higher than the melting ranges of their respective crude waxes. When they are heated to >85 °C, their color changes to dark brown. These waxes become very hard (similar to plastics). The fine crystal structures exhibited in the photomicrographs in Figure 7a and b were smaller than the crystals of the corresponding crude waxes.

Table 7a sums the carbon, hydrogen, sulfur, and oxygen analyses of the waxes of deposits  $\delta\text{A}$ ,  $\delta\text{B}$ , and  $\delta\text{C}$ . Their H/C ratios are 1.92–2.00 and are greater than those of their parent crude waxes (except for the  $\delta\text{B}$  wax). There was negligible nitrogen present (<0.1%) in these waxes, similar to their parent crude waxes. The sulfur and oxygen contents in the  $\delta\text{A}$  wax were less than those of other waxes. There was a higher sulfur content in  $\delta\text{B}$  wax comparable to its parent crude wax. This may partially explain the reason for its lower H/C ratio than the H/C ratio of its crude wax.  $\delta\text{C}$  wax contains both



(a)



(b)

**Figure 7.** Micrographs of waxes isolated from crude oils (a) and associated deposits (b) (20 $\times$  magnification).

higher S% (>1%) and higher O% (~1%) in three waxy-deposit waxes. However, its sulfur content is lower than in its parent crude wax, and its H/C ratio is higher than the H/C ratio of its parent crude wax. Based on FTIR spectra, the waxy-deposit waxes contain ~20% greater straight-chain methylene content than do their parent crude waxes (see Table 9 and Figures 4 and 5). These structural differences are confirmed by the  $^{13}\text{C}$  NMR spectra (Figure 8). The fact that few peaks are observed in their  $^{13}\text{C}$  NMR spectra implies that less-branched chains exist in the structure of waxy-deposit waxes.

Figures 9–11 present HTSD chromatograms of both waxy-deposit waxes and their parent crude waxes, and these show the differences in carbon number distribution. Waxy-deposit waxes contain very little material with a chain length of less than  $\text{C}_{30}$ , with the majority of components falling in the  $\text{C}_{31}$ – $\text{C}_{60}$  range. The  $\text{C}_{37}$ – $\text{C}_{48}$  chains were particularly prominent, typically constituting >30% of the waxes. In contrast, the carbon number range of  $\text{C}_{18}$ – $\text{C}_{32}$  dominates the distribution in all the crude waxes. Paraffin and so-called fine crystalline waxes are both predominantly long-chain *n*-al-

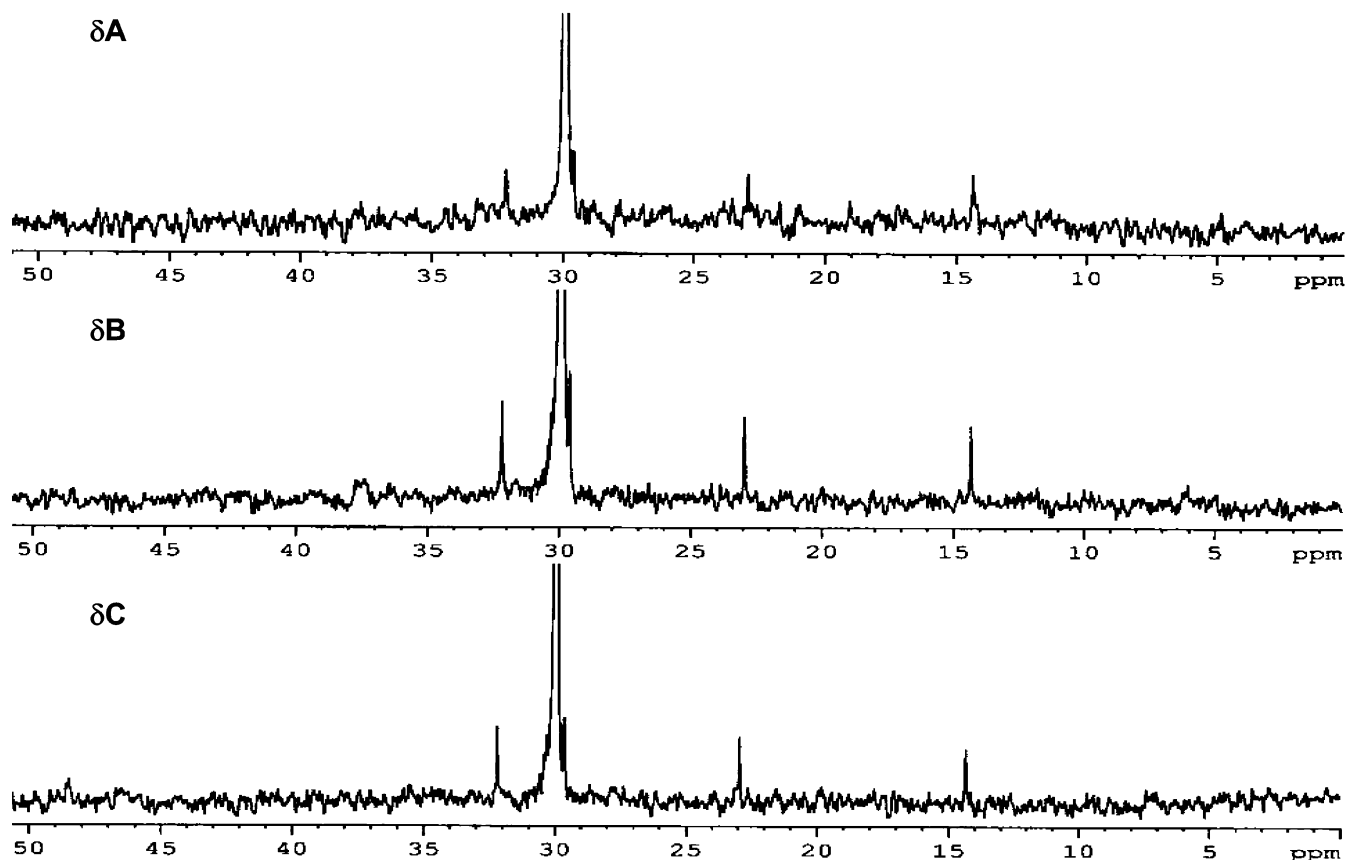


Figure 8.  $^{13}\text{C}$  NMR spectra of waxes isolated from wax deposits.

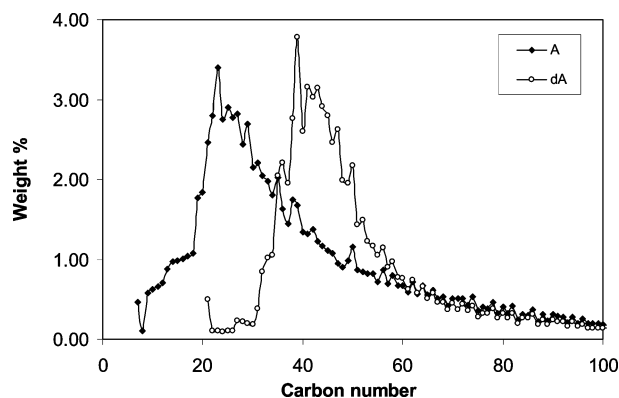


Figure 9. Carbon number distribution from HTSD of A and  $\delta\text{A}$  waxes.

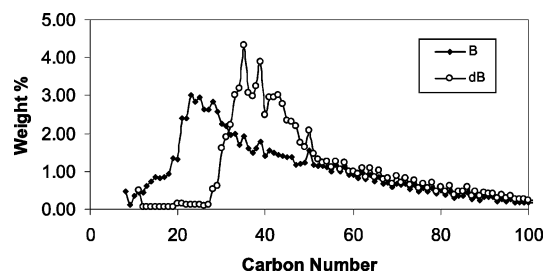


Figure 10. Carbon number distribution from HTSD of B and  $\delta\text{B}$  waxes.

kanes; however, fine crystalline waxes have much-greater molecular weights. The common commercial paraffin waxes have molecular weights of 360–420 (carbon number of 26–30 ( $\text{C}_{26}$ – $\text{C}_{30}$ )). The paraffin waxes

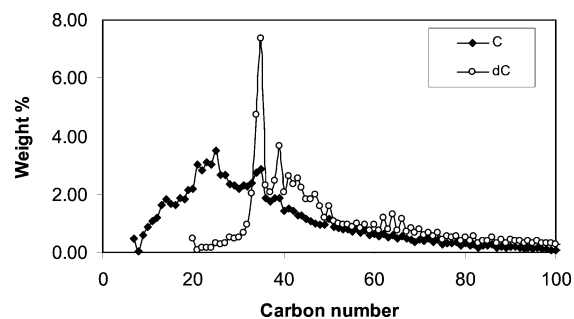
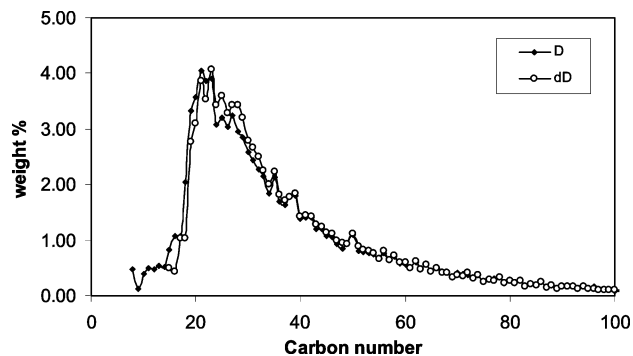


Figure 11. Carbon number distribution from HTSD of C and  $\delta\text{C}$  waxes.

also can be of a greater molecular weight ( $\sim 600$ ) with higher melting ranges. The molecular weight of commercial microcrystalline waxes is 580–700 (carbon number of 41–50 ( $\text{C}_{41}$ – $\text{C}_{50}$ )).<sup>34</sup> The waxy-deposit waxes in this study were relatively long, straight-chain, fine crystalline waxes that possess higher melting points and greater molecular weights than their parent crude waxes. Undoubtedly, their high molecular weights and melting points confer a reduced solubility on them as the temperature is reduced, thus making them precipitate to form deposits. When heated, they changed color and became plastic waxes, which implies that they will be difficult to remove from pipelines through heat treatments.

**3.2.3. Properties of Compositions of Asphaltenic-Deposit Waxes.** Unlike the waxes isolated from waxy deposits, the two waxes from asphaltenic deposits are light yellow, similar to pure paraffin wax. The melting range of  $\delta\text{E}$  wax is in the range of 40–50 °C, similar to



**Figure 12.** Carbon number distribution from HTSD of D and  $\delta$ D waxes.

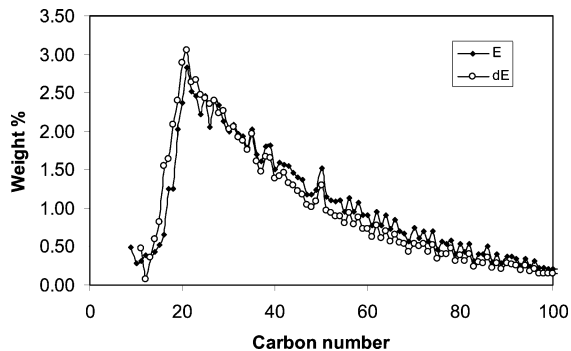


**Figure 13.** Carbon number distribution from HTSD of E and  $\delta$ E waxes.

its parent E wax (see Table 6). No clear crystal structure can be observed in the  $\delta$ E wax. The melting range of wax from  $\delta$ D alkanes is similar to that of its parent crude D wax. In  $\delta$ D wax, some fine crystal structure was observed, which probably results in its broad and high melting points.<sup>34</sup> When heated, these two waxes melt but do not become discolored. The carbon, hydrogen, sulfur, and oxygen analyses of  $\delta$ D and  $\delta$ E waxes are given in Table 7b. The H/C ratio of asphaltenic-deposit waxes was lower than that of their parent crude waxes.  $\delta$ D wax contains relatively lower heteroatomic content, whereas  $\delta$ E wax contained  $\sim$ 1%–5% heteroa-

toms. Both asphaltenic-deposit waxes also showed ca. 10% greater straight-chain methylene content than their parent crude waxes; this difference is considerably less than the difference between waxy-deposit waxes and their crude waxes.

HTSD results that compare asphaltenic-deposit waxes and their parent waxes are shown in Figures 12 and 13, and the similarities in the carbon number distributions are remarkable. Clearly, the *n*-alkanes in these crude waxes coprecipitate in asphaltenic deposits with no selectivity to higher carbon number, in stark contrast with what occurs in waxy deposits that were studied. E and  $\delta$ E <sup>13</sup>C NMR spectra are compared in Figure 14. The strong conformance of these two spectra further confirms the structural and distributional identity of the alkanes in waxes from crude versus asphaltenic deposits. Deposits  $\delta$ D and  $\delta$ E contain 4% waxes, much less than that in their corresponding waxy deposits. The wax fractions in these deposits seem to coprecipitate with asphaltenes, perhaps simply as occluded oil and not because of higher carbon number or molecular weight of the wax fraction.

**3.2.4. Summary of Analyses of Wax Fractions.** The properties and compositions of crude waxes, waxy-deposit waxes, and asphaltenic-deposit waxes were studied in this paper. The following conclusions can be reached:

(1) The major constituents of the crude waxes studied are C<sub>18</sub>–C<sub>32</sub> alkanes. Their melting range is significantly lower than waxy-deposit waxes and is similar to that of asphaltenic-deposit waxes. The branching degree of the methylene chain of crude waxes was significantly higher than that of waxy-deposit waxes. The molecular weight of crude waxes was less than that of the waxy-deposit waxes and similar to that of the asphaltenic-deposit waxes.

(2) The waxy-deposit waxes studied have high melting point ranges (70–90 °C), high straight-chain methylene content, and high molecular weight. Their carbon number distribution is significantly higher than that of crude waxes. Their major constituents are C<sub>37</sub>–C<sub>48</sub>.

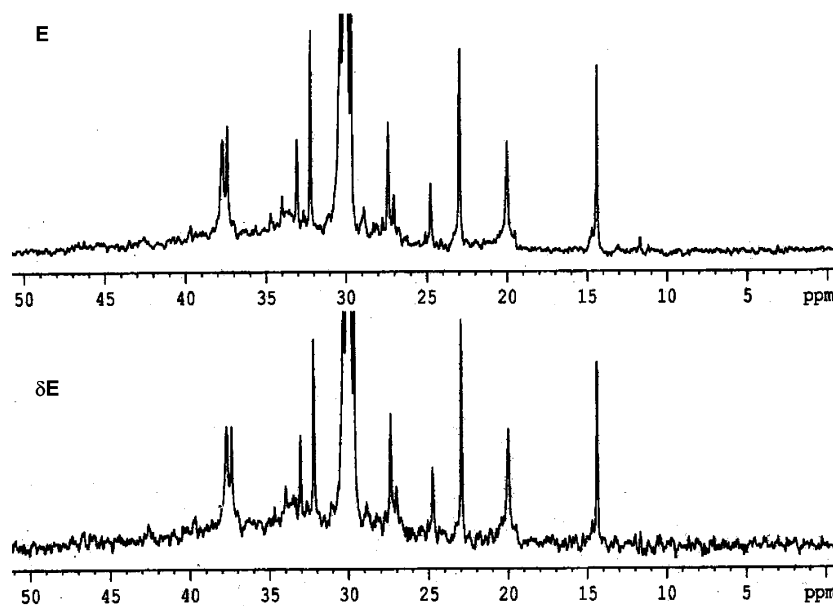


**Figure 14.** <sup>13</sup>C NMR spectra of waxes isolated from crude E and the associated deposit.

**Table 10. Properties of Asphaltenes from Parent Crude Oils and Associated Deposit Asphaltenes (a) in Wax Deposits and (b) in Asphaltenic Deposits**

property	sample C	sample $\delta$ C	sample D	sample $\delta$ D	sample E	sample $\delta$ E
(a) Wax Deposits						
weight in sample (%)	13.29	6.12				
molecular weight (da)	2693	3367				
H/C ratio	1.26	1.37				
N/C ratio	0.024	0.021				
S/C ratio	0.021	0.019				
O/C ratio	0.024	0.023				
C (%)	81.98	81.41				
H (%)	8.60	9.3				
N (%)	2.30	2.03				
S (%)	4.54	4.07				
O (%)	2.64	2.48				
Ni (%)	0.047	0.077				
V (%)	0.072	0.11				
Fe (%)	0.034	0.081				
sum (%)	100.06	99.29				
appearance	particles, shiny	particles, dull				
(b) Asphaltenic Deposits						
weight in sample (%)		0.50	55.71	6.49	27.41	
molecular weight (da)		1171	3673	2886	4253	
H/C		1.38	0.90	1.1	1.04	
N/C			0.007	0.017	0.020	
S/C		0.005	0.007	0.022	0.027	
O/C		0.015	0.022	0.013	0.019	
C (%)		84.97	87.82	83.31	81.50	
H (%)		9.75	6.55	7.64	7.025	
N (%)		<0.5	0.72	1.65	1.87	
S (%)		1.2	1.73	4.85	5.98	
O (%)		1.7	2.57	1.4	2.01	
Ni (ppm)		<60	84	0.034	0.043	
V (%)		0.016	0.032	0.36	0.47	
Fe (ppm) <sup>a</sup>		<60	<129	<59	0.31%	
sum (%)		97.62	99.39	98.85	98.38	
appearance		particles, some shiny	particles, shiny	particles, shiny	particles, shiny	

<sup>a</sup> Values expressed in units of parts per million (ppm), unless noted otherwise.

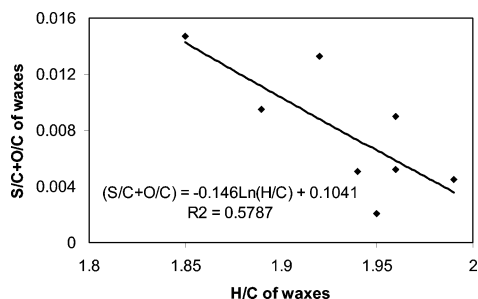


**Figure 15.** Sulfur and oxygen content in waxes from deposits as a function of the H/C ratio of the waxes.

(3) The asphaltenic-deposit waxes have melting point ranges and carbon number distributions similar to their parent crude waxes. Asphaltenic-deposit waxes perhaps are one of the fractions in the occluded oil compositions that are simply coprecipitated with asphaltenes.

(4) With all wax fractions studied, the heteroatom content in waxes was related with the heteroatom content in the original crude oils. The H/C ratio of the waxes shows a correlation with the amount of heteroatom content in the waxes (Figure 15).

**3.3. Asphaltene Fraction Analysis.** It is widely reported that asphaltene precipitation is closely related to asphaltene aggregation.<sup>1,4,5,8,18,45</sup> The aggregation of asphaltenes is typically attributed to their fused and

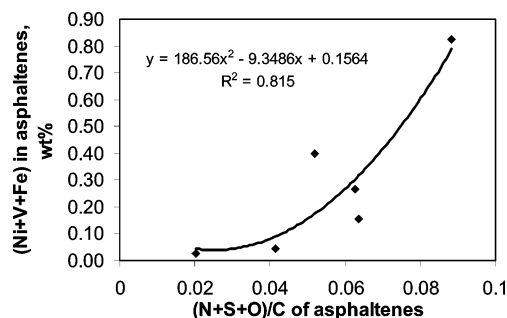


**Figure 16.** Nickel, vanadium, and iron content in asphaltenes as a function of heteroatom content in asphaltenes.

**Table 11. Weight Percentages of Aromatic Carbon and Polar Functional Groups of Asphaltenes in Crudes and Deposits, Based on FTIR Analysis**

sample	C/H ratio	Functional Groups (wt %)			
		O-H	N-H	C=O	C=C
C	1.27	0.029	0.266	0.36	65.6
$\delta$ C	1.37	0.040	0.166	0.31	56.1
D	1.38	0.009	0.099	0.07	45.2
$\delta$ D	0.91	0.036	0.108	0.20	81.0
E	1.10	0.045	0.139	0.17	66.3
$\delta$ E	1.04	0.026	0.141	0.12	67.1

polynuclear aromatic character and to their polar functional groups, which impart their amphiphilic character.<sup>9-11,13,36-38</sup> Sulfur in asphaltenes exists predominantly as thiophenic heterocycles (65%–85%) and sulfidic groups,<sup>46</sup> which are only slightly polar and are not likely to contribute to intermolecular associations. However, a small amount of sulfur speciates as sulfoxide

(45) Cimino, R.; Corraera, S.; Bianco, A. D.; Lockhart, T. P. Solubility and Phase Behavior of Asphaltenes in Hydrocarbon Media. In *Asphaltenes: Fundamentals and Applications*; Sheu, E. Y., Mullins, O. C., Eds.; Plenum Press: New York, 1995; p 97.

Table 12. Apparent FTIR Integrated Absorption Intensities of Selected Functional Groups from Model Compounds<sup>a</sup>

compound	group type	frequency (cm <sup>-1</sup> )	absorption intensity, $\epsilon$ (L mol <sup>-1</sup> cm <sup>-1</sup> )
O-H Functional Group			
1-naphthol	phenol	3580	13200
di- <i>tert</i> -butylphenol	phenol	3580	16700
N-H Functional Group			
carbazole	pyrrole	3462	11900
C=O Functional Group			
cyclohexaneacetic acid	carboxyl (sym + asym)	1707, 1750	26900
cyclohexanecarboxylic acid	carboxyl (sym + asym)	1704, 1750	27900
Aromatic C=C Functional Group			
benzoic acid	carboxyl carboxyl	1600	800
benzoyl BA		1600	800

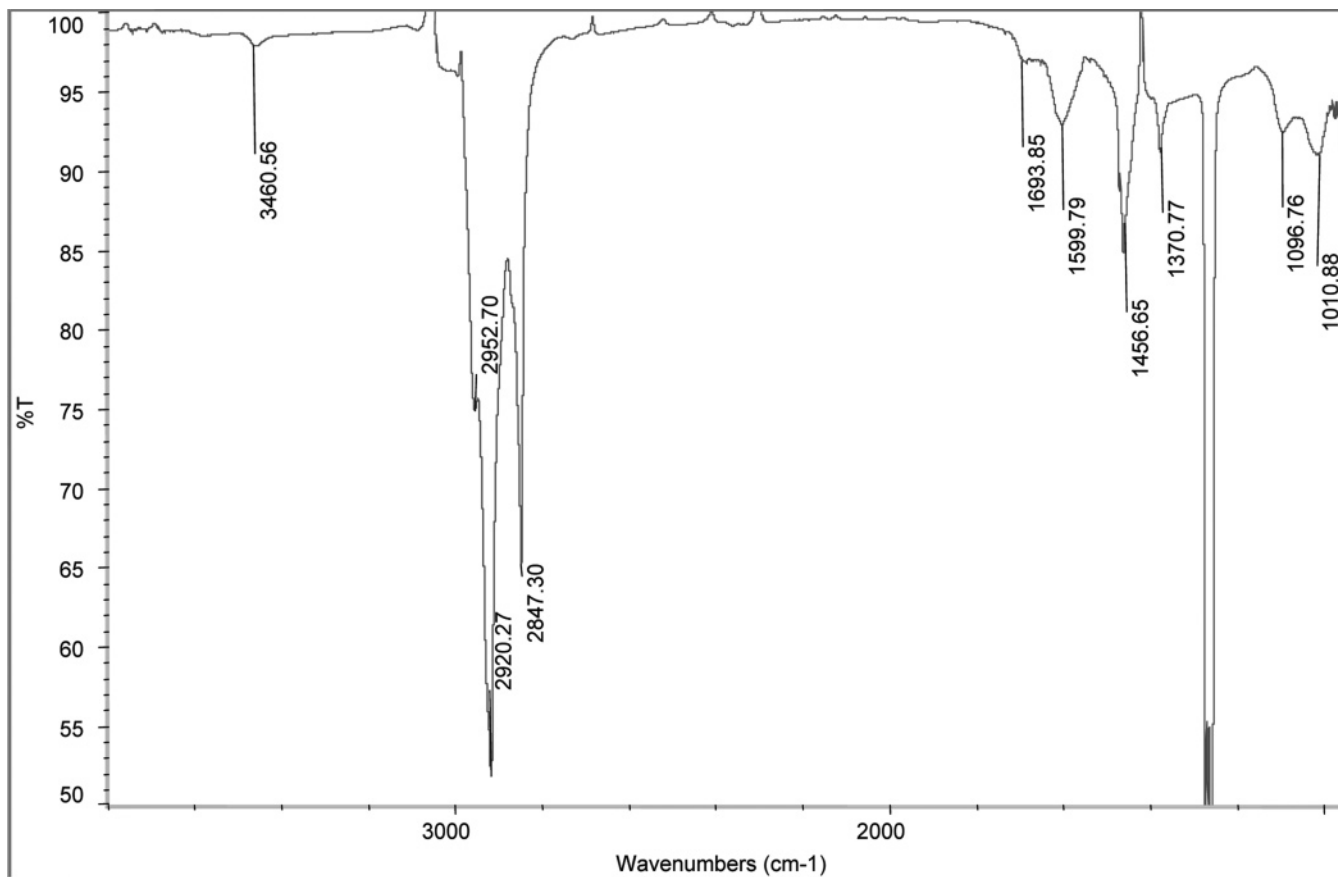
<sup>a</sup> From ref 47.

Figure 17. Fourier transform infrared (FTIR) spectrum of asphaltenes isolated from crude oil D.

and are strongly polar. Nitrogen in asphaltenes exists in pyrrolic, pyridinic, and quinolinic groups, whereas oxygen is present primarily in phenolic, carbonyl, carboxylic, and ether. The oxygen- and nitrogen-containing groups are believed to be those moieties primarily responsible for strong intermolecular associations through hydrogen bonding. The precise structures and mechanisms associated with aggregation and precipitation in petroleum has eluded petroleum researchers for many years.<sup>17-20,36-39</sup>

Six asphaltene samples were isolated from crude oils and their respective deposits. Parts a and b in Table 10 summarize the C, H, N, O, and S elemental analyses, heavy metal analyses, and molecular weight (determined by VPO) of crude and deposit asphaltenes.  $\delta$ C asphaltenes were isolated from a waxy deposit, whereas  $\delta$ D and  $\delta$ E asphaltenes were isolated from asphaltenic

deposits. From Table 10a, it is found that the H/C ratio of  $\delta$ C asphaltenes was higher than the corresponding H/C of C asphaltenes, whereas the nitrogen, sulfur, and oxygen contents of  $\delta$ C asphaltenes were all lower than those of the parent asphaltenes. In contrast, the H/C ratio of  $\delta$ E asphaltenes was less than that of its parent asphaltenes, and the H/C ratio of  $\delta$ D asphaltene was much lower than that of its corresponding crude asphaltene, whereas all heteroatom contents were higher for both asphaltenes. Thus, the waxy-deposit ( $\delta$ C) asphaltenes were more aliphatic and less polar than their corresponding crude asphaltenes, whereas the asphaltenic-deposit ( $\delta$ D,  $\delta$ E) asphaltenes were more

(46) Mullins, O. C. Sulfur and Nitrogen Molecular Structures in Asphaltenes and Related Materials Quantified by XANES Spectroscopy. In *Asphaltene: Fundamentals and Applications*; Sheu, E. Y., Mullins, O. C., Eds.; Plenum Press: New York, 1995; pp 53-96.

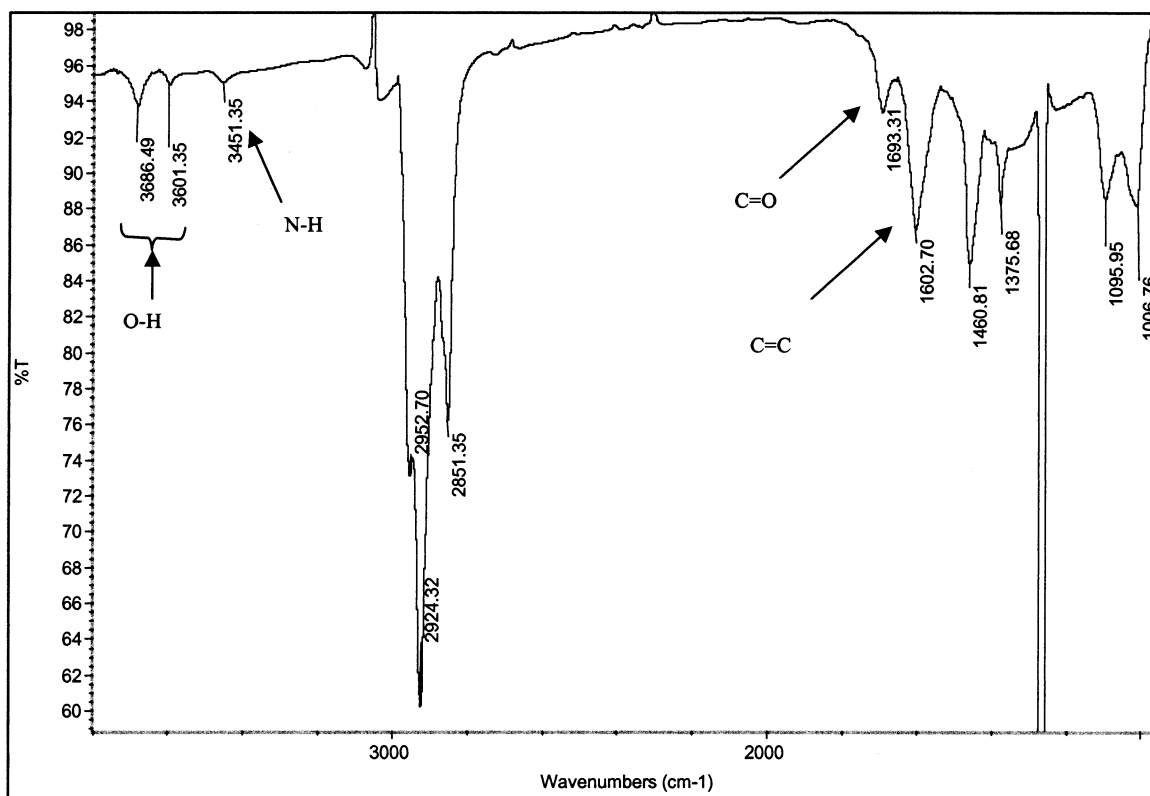


**Figure 18.** FTIR spectrum of asphaltene isolated from deposit  $\delta$ D.

aromatic and polar than their crude asphaltene. The metal contents both in waxy-deposit ( $\delta$ C) asphaltene and in asphaltene-deposit ( $\delta$ D and  $\delta$ E) asphaltene were greater than those in their original crude asphaltene. Figure 16 shows that metal contents in asphaltene correlate well with their heteroatom contents. Finally, VPO data in chlorobenzene indicated that asphaltene-deposit asphaltene possess 1.5–3 times higher apparent molecular weights than their respective crude asphaltene. Compared with asphaltene-deposit asphaltene, waxy-deposit asphaltene ( $\delta$ C) has an apparent molecular weight that is 1.2 times greater than its parent asphaltene.

Apparent functional group concentrations for the asphaltene fractions from FTIR analysis are given in Table 11. The weight percentages of these functional groups were obtained from apparent integrated molar absorptivities ( $\epsilon$ ) of these functional groups in model compounds<sup>47</sup> (see Table 12). The FTIR spectra of D and  $\delta$ D asphaltene are shown in Figures 17 and 18, respectively. The concentrations of aromatic carbon ( $1600\text{ cm}^{-1}$ ), carboxyl ( $1690\text{ cm}^{-1}$ ), and phenolic OH ( $3600\text{ cm}^{-1}$ ) groups in  $\delta$ D asphaltene are all clearly greater than those in the parent D asphaltene. This is reflected in Table 11, where the carboxyl concentration is 3 times higher, and the phenolic OH concentration is 4 times higher, in  $\delta$ D asphaltene, compared to its parent crude D asphaltene. All of these functional groups are strongly hydrogen bound, and it seems plausible that hydrogen-bond interactions may drive aggregation and precipitation, producing an asphaltene deposit that is much richer in these functional groups.

(47) McLean, J. D.; Kilpatrick, P. K. Comparison of Precipitation and Extrography in the Fractionation of Crude Oil Residua. *Energy Fuels* **1997**, *11* (3), 570–585.

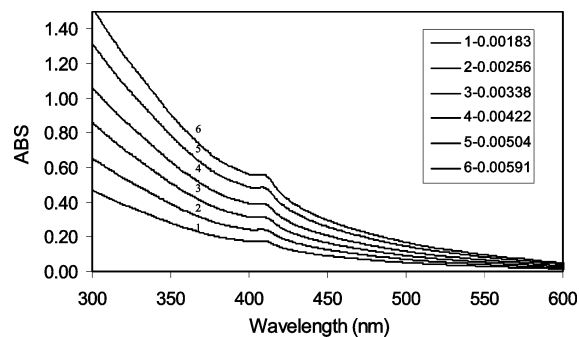


**Figure 19.** UV absorbance versus wavelength of asphaltene isolated from crude oil C and dissolved in toluene as function of concentration.

The remaining oxygen in both  $\delta$ D and D likely speciate as ether oxygen, possibly reflected in the absorbance at  $1010\text{ cm}^{-1}$ , which is relatively nonpolar, compared to the groups discussed previously. With crude E and its corresponding deposit  $\delta$ E, the concentrations of polar groups were not significantly different. Noting that this asphaltene deposit ( $\delta$ E) had a different appearance than  $\delta$ D, one wonders if, based on the chemical information, the mechanism of precipitation and deposition may be somewhat different.

Asphaltene solubility in T/H mixtures was determined by UV–visible spectra. Typical UV–visible spectra of asphaltene are shown in Figure 19. There is a noticeable absorbance peak near 408 nm, and this Soret band is attributed to metalloporphyrin.<sup>48</sup> To minimize the influence of the UV absorbance of toluene, the molar absorptivity at 450 nm was chosen to determine the concentration of asphaltene solutions.<sup>49</sup> Table 13 pre-

(48) Sugihara, J. M.; Bean, R. M. *J. Chem. Eng. Data* **1962**, *7*, 269.

Table 13. Beer–Lambert Calibration of Ultraviolet (UV) Spectra for Crude-Oil and Deposit Asphaltenes

sample	fraction	correlation coefficient, $R^2$	slope	resource
C	$Y = 50.635x - 0.0048$	0.9979	50.635	crude
$\delta C$	$Y = 64.799x - 0.0198$	0.9959	64.799	wax deposit
D	$Y = 85.563x - 0.0014$	0.9933	85.563	crude
$\delta D$	$Y = 73.416x - 0.017$	0.9799	73.416	asphaltenic deposit
E	$Y = 92.016x - 0.0114$	0.9947	92.016	crude
$\delta E$	$Y = 46.185x - 0.0181$	0.9978	46.185	asphaltenic deposit

Table 14. Solubility of Asphaltenes in Toluene–*n*-Heptane Mixtures

sample	Solubility (%)				
	70% toluene	60% toluene	50% toluene	40% toluene	30% toluene
C	10.71	3.04	1.62	0.60	0.27
$\delta C$	4.00	1.99	0.83	0.40	0.06
D	10.88	7.68	4.61	2.93	0.79
$\delta D$	0.17	0.11	0.07	0.04	0.01
E	10.14	3.06	1.69	0.72	0.32
$\delta E$	1.86	1.52	0.65	0.11	0.02

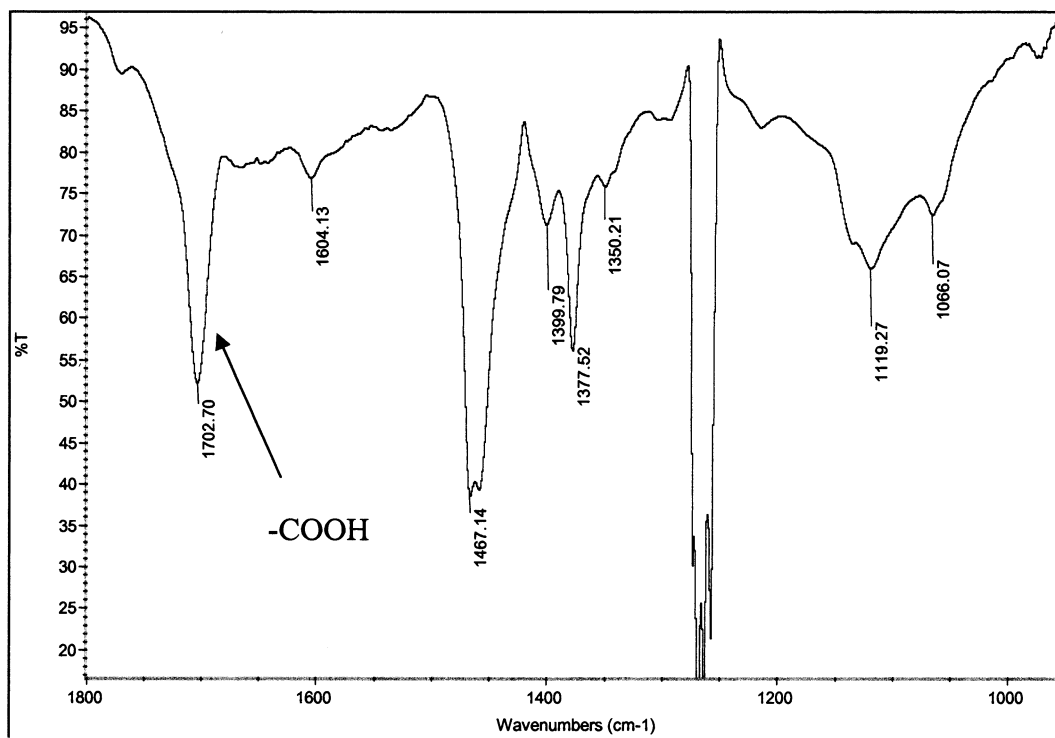
sents the formulas and coefficients of the calibration curves for crude and deposit asphaltenes. The UV–visible absorbance of diluted asphaltene–toluene solutions are well described by the Beer–Lambert law. The linear correlation coefficients of these calibrations were  $>0.993$  (with the exception of a value of 0.97 in the case of  $\delta D$ ), thus providing an accurate method to quantify the concentrations of asphaltenes in toluene. Saturated solutions of asphaltenes dissolved in T/H mixtures were prepared, filtered, and then diluted into the Beer's law region. The asphaltene concentrations of these saturated solutions were then obtained according to a calibration curve. Table 14 summarizes the solubility results for crude and deposit asphaltenes. Comparing three asphaltenes ( $\delta C$ ,  $\delta D$ , and  $\delta E$ ), the solubility of waxy-deposit asphaltene ( $\delta C$ ) was higher than the solubility of asphaltenic-deposit asphaltenes  $\delta D$  and  $\delta E$ . The

Table 15. Elemental Analysis of Fractions Isolated from Deposit  $\delta F$ 

fraction	heptane dissolved	methylene chloride
C (%)	67.94	64.79
H (%)	10.41	9.63
N (%)	2.66	2.8
S (%)	2.84	0.31
O (%)	16.12	19.77
H/C ratio	1.84	1.78
N/C ratio	0.033	0.037
S/C ratio	0.015	0.001
O/C ratio	0.178	0.229
appearance	dark orange liquid	dark stick solid

solubility of all deposit asphaltenes was much lower than the solubility of their respective crude asphaltenes in T/H mixtures. Deposit  $\delta D$  showed very low solubility in T/H mixture, presumably because of its high aromaticity and high polarity, resulting in strong association and aggregation. Lower solubilities of  $\delta C$  and  $\delta E$  asphaltenes, as compared to their respective crude asphaltenes, also demonstrate that these deposit asphaltenes possess a stronger tendency toward association/aggregation than their respective crude asphaltenes. This suggests that deposit asphaltenes cannot easily redissolve in solvents or crude oil, because of the size of aggregates and particles resulting from the precipitation from crude oils.

According to the aforementioned results, we conclude the following in this study:

Figure 20. FTIR spectrum of deposit isolated from deposit  $\delta F$ .

(1) Asphaltenic-deposit asphaltenes have a lower H/C ratio and higher aromaticity than their respective crude asphaltenes.

(2) Deposit asphaltenes showed higher molecular weights, which are indicative of larger aggregate sizes in chlorotoluene, than their parent crude asphaltenes.

(3) Deposit asphaltenes have lower solubility in T/H mixtures than their respective parent crude asphaltenes.

(4) Some properties of waxy-deposit asphaltenes show different trends than asphaltenic-deposit asphaltenes. This difference perhaps implies that asphaltenes isolated from the waxy deposit also as occluded oil coprecipitated with the waxy deposit, although they have relative higher molecular weight or lower solubility.

**3.4. Properties and Composition of Deposit  $\delta F$ .** In the crude and deposit samples collected,  $\delta F$  was a very unusual deposit that was obtained from a pipeline pigging. Its elemental analysis yielded a higher H/C ratio (2.05) and higher oxygen content of 19.66% (see Table 2), compared to those of other deposits (Table 15). Approximately 63 wt % of the constituents in  $\delta F$  could not be dissolved in hot heptane in a Soxhlet extractor (Table 4); however, they did subsequently dissolve in methylene chloride. Unlike higher-molecular-weight waxes discussed previously, these results demonstrate that the fraction dissolved in methylene chloride is not asphaltenic, because of its high H/C ratio (1.78). The heptane-soluble fraction also contained 16.12% oxygen. Figure 20 presents the FTIR spectrum of the fraction in  $\delta F$ , which did not dissolve in hot heptane. The large carbonyl absorption at  $1702\text{ cm}^{-1}$  and the phenolic peak at  $3450\text{ cm}^{-1}$  were integrated to give 0.40% OH and 2.88% C=O, the highest such values in all of the fractions isolated from either crudes or deposits. All the values may be somewhat low, because of the large value of the integrated molar absorbance intensity utilized for phenolic and carboxyl moieties; values obtained from fused aromatic ring carboxylic functional groups may be lower and yield a truer measure of the acid and phenol content in these samples. These results indicate that the majority fraction in  $\delta F$  contains a significant amount of carboxylic acid and aliphatic acid, which is different from that observed for waxy-deposit waxes and asphaltenic-deposit waxes.

#### 4. Conclusion

In this study, we have carefully analyzed the chemical compositions and molecular properties of five crude oils

and their corresponding deposits, to discern the nature of the deposition process and determine whether there is evidence of coprecipitation of (or synergy between) paraffin waxes and asphaltenes. Three of the deposits—those from crudes A, B, and C—were clearly paraffin wax deposits. The evidence clearly indicates that the precipitation and deposit was induced by the phase separation of a wax component that is more paraffinic and has a higher average carbon number than that of the parent crude oil wax. This was verified in a variety of chemical and physical ways, including elemental analysis, high-temperature simulated distillation (HTSD), polarizing microscopy, and Fourier transform infrared (FTIR) spectroscopy. The remaining components in these wax deposits—entrained oil, asphaltenes, and some minor amount of inorganic solids—seemed to have the same chemical composition and molecular distribution of these same components in the parent crude oil, i.e., there is no evidence for synergy in precipitation. Similarly, the other two organic deposits studied—those from crudes D and E—were clearly asphaltenic deposits. There was clear evidence that the asphaltenes isolated from these deposits had a much lower solubility in mixtures of toluene and heptane than the corresponding asphaltenes from the parent crude oils, indicating that the mechanism of deposition was related to a phase separation of these more sparingly soluble fractions of the original asphaltenes. Detailed chemical and physical analyses suggested that the origins of these decreased solubilities were some combination of increased aromaticity and polarity of these fractions. A sixth deposit studied was quite unusual and seemed to be a naphthenic acid deposit (sample  $\delta F$ ). In summary, asphaltenes and waxes do not interact synergistically and coprecipitate in solid organic deposits.

**Acknowledgment.** This work was supported by a contract from Shell International Exploration and Production Technology and Research Company. We express our appreciation to Dr. Nick Fuex, Dr. Matthew Flannery, Dr. Sheila Dubey, Dr. Artur Stankiewicz, and Dr. George Broze for providing many good suggestions and assisting with much of the data generation. We also thank Dr. Hanna Gracz for her assistance in performing the  $^{13}\text{C}$  and  $^1\text{H}$  NMR spectroscopy measurements, and we thank our two undergraduate researchers Bojan Prokic and Karen Lu, who contributed to this study.

EF050022C

(49) Yang, X. L.; Hamza, H.; Czarnecki, J. *Energy Fuels* **2004**, *18*, 770–777.